Pharm Res (2014) 31:360–372
DOI 10.1007/s11095-013-1165-6

RESEARCH PAPER

Development of a High Efficiency Dry Powder Inhaler: Effects of Capsule Chamber Design and Inhaler Surface Modifications

Srinivas R. B. Behara • Dale R. Farkas • Michael Hindle • P. Worth Longest

Received: 24 April 2013 / Accepted: 28 July 2013 / Published online: 16 August 2013

ABSTRACT

Purpose The objective of this study was to explore the performance of a high efficiency dry powder inhaler (DPI) intended for excipient enhanced growth (EEG) aerosol delivery based on changes to the capsule orientation and surface modifications of the capsule and device.

Methods DPIs were constructed by combining newly designed capsule chambers (CC) with a previously developed three-dimensional (3D) rod array for particle deagglomeration and a previously optimized EEG formulation. The new CCs oriented the capsule perpendicular to the incoming airflow and were analyzed for different air inlets at a constant pressure drop across the device. Modifications to the inhaler and capsule surfaces included use of metal dispersion rods and surface coatings. Aerosolization performance of the new DPIs was evaluated and compared with commercial devices.

Results The proposed capsule orientation and motion pattern increased capsule vibrational frequency and reduced the aerosol MMAD compared with commercial/modified DPIs. The use of metal rods in the 3D array further improved inhaler performance. Coating the inhaler and capsule with PTFE significantly increased emitted dose (ED) from the optimized DPI.

Conclusions High efficiency performance is achieved for EEG delivery with the optimized DPI device and formulation combination producing an aerosol with MMAD < 1.5 μm, $FPF_{<5\mu m/ED}$ > 90%, and ED > 80%.

S. R. B. Behara • D. R. Farkas • P. W. Longest (✉)
Department of Mechanical and Nuclear Engineering
Virginia Commonwealth University
401 West Main Street, P.O. Box 843015
Richmond, Virginia 23284-3015, USA
e-mail: pwlongest@vcu.edu

S. R. B. Behara • M. Hindle • P. W. Longest
Department of Pharmaceutics, Virginia Commonwealth University
Richmond, Virginia, USA

KEY WORDS 3D rod array · excipient enhanced growth · high efficiency DPI · low surface energy coatings · PTFE coating

ABBREVIATIONS

3D	Three-dimensional or three-dimensional rod array constructed of resin
3Dm	Three-dimensional rod array constructed of metal
AL	Aerolizer
AS	Albuterol sulfate
CC	Capsule chamber
CFD	Computational fluid dynamics
CV	Coefficient of variation
DPI	Dry powder inhaler
ED	Emitted dose
EEG	Excipient enhanced growth
FPF	Fine particle fraction
HH	HandiHaler
HPLC	High-performance liquid chromatography
HPMC	Hydroxypropyl methylcellulose
MMAD	Mass median aerodynamic diameter
MT	Mouth-throat
NDSD	Non-dimensional specific dissipation
NGI	Next generation impactor
PDA	Photo diode array
PTFE	Polytetrafluoroethylene
R^2	Coefficient of determination
SD	Standard deviation

INTRODUCTION

Dry powder inhalers (DPIs) are an increasingly popular platform for delivering inhaled medications to the lungs (1–3). Advantages of DPIs compared with other modes of aerosolization include stable formulations, automatic coordination

between inhalation and dose delivery, low cost, and a wide variety of design attributes that can be used to optimize performance. However, drug delivery to the lungs from DPI platforms is known to be inefficient. In a recent review of DPIs (1), fine particle fractions (FPF) of aerosolized particles with sizes less than 5 μm ($FPF_{<5\mu m}$) for both commercial and research devices were in the range of 10–70%. With DPIs, increasing the inhalation airflow rate is typically required to increase the FPF; however, higher flows also increase depositional loss in the mouth-throat (MT) region due to turbulence and inertial impaction (4,5). Depositional losses in the MT for DPIs are typically in the range of 30–95% (2,5–8). Advances such as large porous particles have recently improved DPI performance and reduced MT deposition to approximately 30–40% for some applications (9,10).

A new method to improve the performance of DPIs is the application of excipient enhanced growth (EEG) technology (11,12). In this approach, aerosols are generated from submicrometer particles that are composed of a drug and a hygroscopic excipient. The small size of the aerosol particles minimizes deposition in the device and extrathoracic airways. The size of the particles increases in the warm and humid lung environment due to inclusion of the hygroscopic excipient and associated water uptake, resulting in lung deposition of the aerosol. Previous studies with spray generated aerosols and EEG delivery have demonstrated low MT deposition (12), significant increase in aerosol size when entering the lungs (11,13,14), *in vitro* deposition of the aerosol within the airways (15), and the potential to target deposition to regions of the lungs (15).

Implementation of the EEG approach with a DPI platform requires the generation of an aerosol with a high submicrometer fine particle fraction ($FPF_{<1\mu m}$) that will have very low MT deposition. Developing a high efficiency DPI for EEG delivery is challenging because both cohesive and adhesive forces increase relative to aerodynamic forces as the primary particle size is reduced (16–18). For submicrometer primary particles, device emptying and deaggregation efficiency are expected to be low when using current commercial inhalers and formulation methods. To produce a highly effective DPI that can overcome the expected challenges of forming a submicrometer aerosol, both formulation and inhaler design aspects must be addressed.

Considering the development of an EEG formulation, Son *et al.* (19) implemented a spray drying process to form the submicrometer primary combination particles. Optimum spray drying and formulation conditions were determined and the final combination particles contained albuterol sulfate (AS; model drug), mannitol (hygroscopic excipient), L-leucine (dispersion enhancer), and poloxamer 188 (surfactant). Son *et al.* (20) tested the optimum formulation in the commercial Aerolizer® (Novartis, Switzerland) (AL) at an airflow rate of 80 L min^{-1} and reported emitted $FPF_{<5\mu m}$ and $FPF_{<1\mu m}$ values of 95.3% and 28.3%, respectively. Using a previously established MT *in vitro* model (7), extrathoracic depositional losses were found to be less than 5%. The study of Son *et al.* (20) implemented this optimized formulation and evaluated the effects of DPI design on the formation of a submicrometer aerosol and deposition in the MT model. A series of four commercial DPIs and a modified design were considered. The modified device consisted of the capsule chamber (CC) of the HandiHaler® (Boehringer Ingelheim, Germany) (HH) coupled to a new mouthpiece that implemented a novel three-dimensional (3D) rod array to deagglomerate the powder. The modified HH device produced optimal performance with an emitted dose (ED) of 74.2%, emitted $FPF_{<5\mu m}$ and $FPF_{<1\mu m}$ of 97.3% and 38.8%, respectively, and a mass median aerodynamic diameter (MMAD) of 1.1 μm at an airflow rate of 45 L min^{-1}. Using this new device, depositional loss for the optimized formulation in the *in vitro* MT geometry was 2.6%. Longest *et al.* (21) analyzed eight mouthpieces including the 3D rod array employed by Son *et al.* (20) using a combination of CFD modeling and *in vitro* analysis. For carrier-free formulations, a new parameter referred to as the non-dimensional specific dissipation (NDSD) was introduced and found to best correlate with aerosol deagglomeration. The 3D rod array design was found to maximize NDSD and therefore most effectively deagglomerate the carrier-free formulation at both a constant pressure drop and a constant airflow rate based on the eight mouthpieces considered.

One aspect of device design that was not previously considered for a high efficiency EEG DPI is the capsule orientation and associated capsule motion. Different commercial inhalers have implemented various capsule chambers, which control capsule motion. For example in the AL, the capsule spins on its short center axis during operation due to tangential air entry impinging on the outer capsule edges. In the HH, the capsule oscillates on its long axis due to direct fluid impingement and instability. Parallel fluid entry together with a large volume CC makes the capsule rattle and vibrate in the Rotahaler® (GSK, UK). A recent comparative study between these devices demonstrated that one of the reasons for the high variability in the rate of powder emptying (22) and deagglomeration (23) was the volume of the CC. Another comparative study between these devices demonstrated that high deagglomeration efficiency and low variability of the AL at 4 kPa was due to a narrow CC, capsule aperture size and the mechanism of direct air impingement on the capsule (24). Hence, past literature collectively confirms that powder residence time within a device (due to capsule aperture size), capsule movement, and direct impingement of air on the capsule facilitate powder deagglomeration. Considering existing designs, one capsule orientation approach that has not been explored in the literature is alignment of the long capsule axis perpendicular to the flow through the inhaler. It is expected that airflow perpendicular to the long axis of the

capsule will increase the instability of the airflow around the capsule due to the Bernoulli effect and thereby increase vibrational frequency and wall impactions leading to improved initial fluidization of the powder.

Emitted doses for the high efficiency EEG DPIs previously explored are in the range of 70–80% (20). These values are consistent with most state-of-the-art DPI devices that employ conventional aerosol sizes. However, it is known that surface properties can influence adhesion of particles in an inhaler. For example, Podczeck (25) quantified adhesion forces for different types of capsules, pigments used in capsules, and inhaler materials. Selvam *et al.* (26) illustrated varying aerosol detachment from different carrier film types. The effects of detachment from carrier particles based on carrier size, morphology, and surface energy are also well known (27,28). Based on these studies, one potential method to further improve the ED of submicrometer particles from a high efficiency DPI is to apply low surface energy coatings to the capsule and device. The approach of coating the capsule and device with different force control agents to improve ED and aerosol performance has not previously been considered in the scientific literature; except in one very recent study (29) where the capsule and device were coated with a suspension of low surface energy material.

The objective of this study is to explore the development of a high efficiency DPI intended for EEG aerosol delivery based on the effects of a new capsule orientation configuration with different air inlet patterns and low surface energy coatings of the capsule and/or device. The previously optimized powder formulation of Son *et al.* (19) is used in combination with the previously developed 3D rod array mouthpiece. The new CC orients the capsule perpendicular to the flow and includes either one or two air inlets, with the multiple inlets either inline or staggered. All complete devices are tested at a pressure drop of 4 kPa, as recommended by the USP, which generated airflow rates between 40 and 50 L min^{-1}. The effects of four different low surface energy coatings on the capsule and/or inhaler devices are also evaluated, along with the use of metal instead of resin rods in the 3D array. Results are presented in terms of capsule, mouthpiece, and CC drug retention, ED, FPF less than 5 and 1 μm with reference to ED ($FPF_{<5\mu m/ED}$ and $FPF_{<1\mu m/ED}$), and the aerosol MMAD. Performance is compared with two commercial devices as well as previously reported high efficiency DPIs for EEG delivery. Based on previous studies with EEG formulations (19,20), high efficiency performance in this study is considered to include the production of an aerosol with an MMAD of less than 1.5 μm, a $FPF_{<1\mu m/ED}$ above 30%, a $FPF_{<5\mu m/ED}$ above 90%, and an ED of approximately 75% or higher. It is expected that the applied modifications will further enhance performance of the existing EEG DPI platform by increasing deagglomeration and reducing device retention. The design options explored in this study are also valuable for applications to current conventional DPIs that employ larger carrier-based particles, where performance improvement can be significantly increased.

MATERIALS AND METHODS

Materials

Albuterol sulfate USP and magnesium stearate NF were purchased from Spectrum Chemical Co. (Gardena, CA) and City Chemicals Corporation (New York, NY), respectively. Pearlitol® PF-Mannitol was donated from Roquette Pharma (Lestrem, France). Poloxamer 188 (Leutrol F68) was donated from BASF Corporation (Florham Park, NJ). L-leucine and all other reagents were purchased from Sigma Chemical Co. (St. Louis, MO). Hydroxypropyl methylcellulose (HPMC) capsules (size 3) were donated from Capsugel (Morristown, NJ).

Preparation of Excipient Enhanced Growth Formulation

Excipient enhanced growth formulation combination particles were engineered as described by Son *et al.* (19). Briefly, a $20\%^{v}/_{v}$ ethanol in water solution containing 0.5 mg/ml of solids consisting of AS, mannitol, L-leucine and poloxamer 188 in a ratio of $30{:}48{:}20{:}2\%^{w}/_{w}$ was spray dried using a Büchi Nano spray dryer B-90 (Büchi Laboratory-Techniques, Flawil, Switzerland). The spray dryer air flow rate was 120 L min^{-1} and droplets were generated using the 4 μm nozzle diameter at an air inlet temperature of 70°C. The resulting air outlet temperature and spray dryer pressure were 40°C and 35 mbar, respectively. Powder was collected from the electrostatic precipitator and was stored in a desiccator until it was used. The powder yield was about 50–60%. Approximately 1 mg powder was dissolved in 100 ml of deionized water to determine the content uniformity of AS in the formulation using a validated HPLC method ($n=3$).

Inhaler Engineering and Geometries

The inhalers consist of a CC unit and a mouthpiece. The CC is oriented such that the major axis of the capsule is perpendicular to the incoming airflow. This CC is connected to the previously developed downstream mouthpiece containing a 3D rod array (CC-3D). The base inhaler is illustrated in Fig. 1. In previous studies, the CC of the commercial HH was employed in combination with a newly developed mouthpiece containing the 3D rod array to deagglomerate the powder, and both the mouthpiece and rod array were constructed of a resin material. The 3D rod array was found to maximize deagglomeration for a range of airflow rates compared with multiple other designs (20,21).

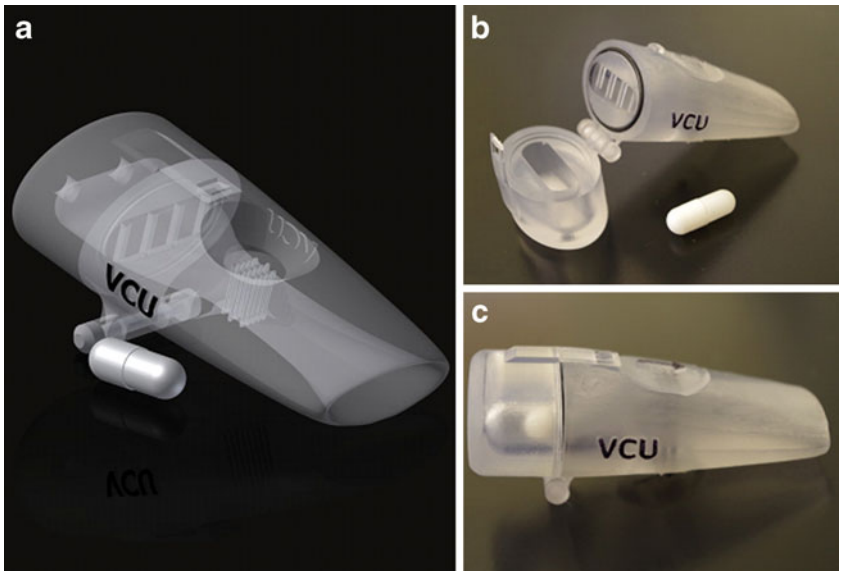

Fig. 1 Images of the CC_1-3D inhaler including (**a**) surface model of the composite device with an internal 3D rod array, (**b**) an opened device for capsule loading with a size 3 capsule, and (**c**) the prototyped device for experimental testing. (**b**) Illustration of the device separated at the interface between the capsule chamber (CC) analyzed in this study and the previously optimized downstream flow passage (mouthpiece) with a 3D rod array.

In the current study, new designs of the CC are explored in order to potentially enhance the initial fluidization of the aerosol and the overall aerosol performance. The basis of the new CC design is to orient the long axis of the capsule perpendicular to the incoming air. Flow that strikes the long axis of the capsule causes instability and results in higher airflow velocities on one side of the capsule body. Based on the Bernoulli equation, the side of the capsule with the highest air velocity will experience the lowest pressure. The resulting pressure difference that is created across the capsule drives the capsule to move toward the low pressure. As the capsule moves, the side of the capsule with the highest velocity and lowest pressure reverses creating an oscillating and/or vibrating motion. It is expected that the perpendicular orientation of the capsule will have a different vibrating frequency compared to the case of air in-line with the capsule major axis, resulting in potentially improved initial fluidization of the powder.

Figure 2 shows the CCs investigated in this study. In order to study the effect of air inlet hole configurations, the dimensions of the CCs were kept constant. The internal width, length and height of all CCs were 6.6, 20.0 and 12.0 mm, respectively (Fig. 2a and b). For the initial design, CC_1, two air

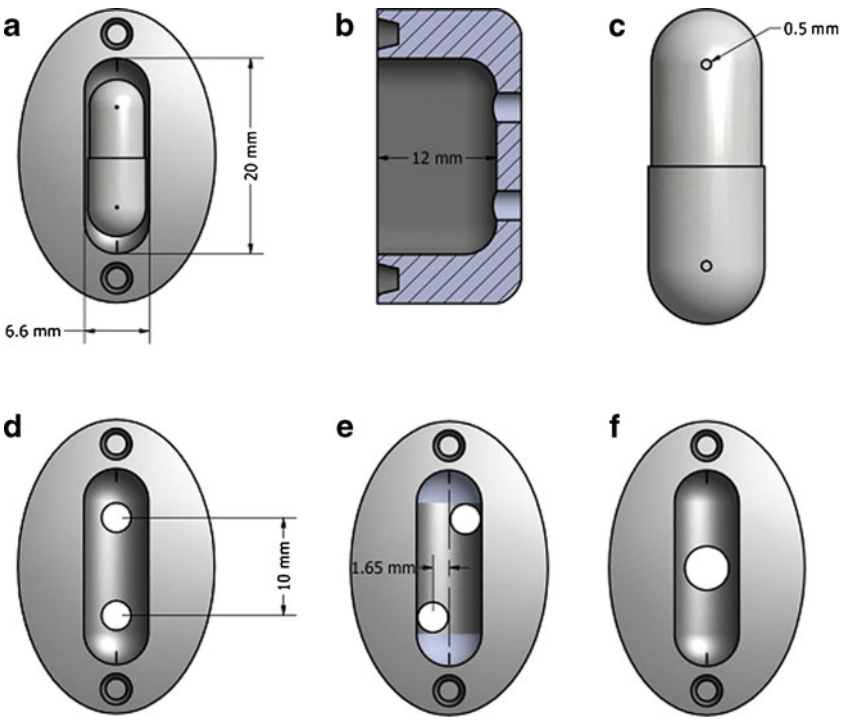

Fig. 2 Images of the capsule chambers: (**a**) top view with dimensions and a size 3 capsule in place, (**b**) side view illustrating height of all capsule chambers, and (**c**) capsule aperture position on the capsule. Air inlet holes differentiate the capsule chambers considered with (**d**) 2 inline inlets (CC_1), (**e**) 2 inlets staggered by 1.65 mm (CC_5), and (**f**) one central inlet (CC_6).

inlets are located in-line at the back of the CC and direct flow perpendicular to the long axis of the capsule (Fig. 1d). Due to instabilities, the capsule can oscillate in a plane perpendicular to the inlet airflow and can also move forward and backward in the CC. In a series of modifications to this chamber, the positions of the air holes were staggered with varying offsets from the centerline. CC_1 (Fig. 2d), CC_2, CC_3, CC_4 and CC_5 (Fig. 2e) have offsets of 0, 0.41, 0.83, 1.24 and 1.65 mm, respectively. An additional design (CC_6) had a single central inlet hole (Fig. 2f).

The size of the air inlet holes varied depending on the inhaler resistance, which was measured using the method developed by Clark and Hollingworth (30). The air inlet holes were mechanically drilled to various diameters using appropriately sized drill bits and the airflow resistance of the device was determined. Using resistance as a function of air inlet hole diameter, the air inlet hole diameters for each CC were calculated from regression equations so as to result in a 4 kPa pressure drop across the device at approximately 45 ± 5 L min^{-1} for $CCs_{1\text{-}6}$ together with the 3D rod array mouthpiece. The diameters of the resulting air inlet holes are shown in Table I.

The inhalers were created using Autodesk Inventor and exported as .STL files to be prototyped. The files were then prepared using 3D Lightyear File Preparation Software. The parts were built using a 3D Systems Viper SLA Prototyper (3D Systems Inc., Rock Hill, SC) using Accura 60 stereolithography resin (3D Systems Inc.). Once the parts were prototyped, they were cleaned using a Proclean SL Part Washer (3D Systems Inc.) and dried in a 3D Systems dryer for approximately 90 min.

Surface Modification Methods

Three surface modifications were investigated: (i) comparison of resin and metal 3D rod arrays, (ii) surface coating the inhaler and capsule using PTFE, and (iii) surface coating of the capsule with low surface energy powders.

The aerosolization performance of a 3D rod array constructed from prototyper resin was compared with an identical 3D array design constructed with metal rods. In addition, the effect of the distance between the exit of the CC and the 3D rod array was investigated to minimize drug deposition during aerosolization.

In a separate study on surface modifications, both capsule and device were coated with a commercial polytetrafluoroethylene (PTFE) suspension (LU™708, Sprayon Products, Cleveland, OH), which is a high contact angle (or low surface energy) material. A suspension of PTFE was sprayed inside the capsule, mouthpiece and CC to form a thin coating. Compressed air was blown through the coated portions until the surface appeared dry.

Finally, in order to minimize retention of the drug within the capsule, the walls of the capsule were pre-coated with a series of powders prior to filling the capsule with the EEG formulation. Two low surface energy materials, L-leucine and magnesium stearate, were tested, together with pre-coating the capsule with the EEG formulation, as a control, in an attempt to decrease the adhesion force on the capsule walls. L-leucine and magnesium stearate were separately triturated using mortar and pestle and sieved using a mesh with 53 micron openings (sieve # 270; Central Scientific Co., Chicago, IL) prior to pre-coating the capsule. In order to coat the

Table I The Effect of Air Inlet Hole Staggering on the Mean Drug Deposition and Aerosolization Performance for CCs 1–5 Coupled with the 3D Rod Array Mouthpiece Tested at a 4 kPa Pressure Drop

Description	CC_1-3D	CC_2-3D	CC_3-3D	CC_4-3D	CC_5-3D
Offset distance (mm)	0.00	0.41	0.83	1.24	1.65
Air inlet hole diameter (mm)	3.16	2.78	3.17	2.78	3.08
Air flow rate (L min^{-1})	50	40	50	43	50
Emitted (%)*	66.2 (1.8)	68.4 (3.6)	67.0 (10.0)	64.9 (17.3)	6.3 (63.9)**
Capsule retention (%)*	13.7 (10.5)	13.5 (17.4)	10.1 (6.7)	14.4 (50.3)	90.4 (5.4)**
Capsule chamber retention (%)	6.1 (17.3)	5.4 (30.3)	12.0 (40.4)	9.8 (81.9)	2.1 (55.1)
Mouthpiece retention (%)*	14.1 (4.4)	12.7 (8.0)	10.9 (21.7)	10.9 (21.2)	1.1 (37.7)**
$FPF_{<5\mu m/ED}$ (%)*	93.8 (0.7)	93.6(1.1)	94.3 (3.0)	89.7 (1.0)	75.3 (16.4)**
$FPF_{<1\mu m/ED}$ (%)*	30.9 (1.9)	32.7 (4.1)	31.7 (3.4)	28.6 (7.3)	20.8 (30.3)**
MMAD (μm)*	1.47(1.22)	1.46 (2.54)	1.44 (0.68)	1.55 (3.76)	1.83 (15.39)**

Batch-1 EEG Formulation Combination Particles Generated by Büchi Nano Spray Dryer (B-90)

Coefficient of variation (%) is shown in parenthesis [$n = 3$]

*$P < 0.05$ significant effect of air inlet staggering on % emitted, capsule & mouthpiece retentions, $FPF_{<5\mu m/ED}$, $FPF_{<1\mu m/ED}$ and MMAD (one-way ANOVA)

**$P < 0.05$ significant difference compared to CC_1-3D (post-hoc Tukey)

capsule walls, a sham actuation procedure was performed to distribute the powder on the walls. In this procedure, 2 mg of the coating powder was placed into the HPMC capsule and the capsule was actuated at 45 L min^{-1} for 5.3 s for an inhaled volume of 4 L using the HH. After the coating process, the capsule head and body were separated and tapped to remove any remaining powder while leaving an adherent and visible layer on the walls of the capsule.

Comparison of Optimized Device Performance with Commercial Inhalers

Aerosolization of the EEG formulation was evaluated in two commercially available dry powder inhalers, AL and HH, together with a modified version of the HH (HH-3D) that had previously been evaluated (20). The aerodynamic particle size distributions of EEG aerosols were determined at 80 L min^{-1} using the AL and 45 L min^{-1} for the HH and its modified version (HH-3D).

Characterization of the Aerodynamic Particle Size Distribution

To characterize the aerodynamic particle size distribution, 2 mg of EEG formulation was weighed and manually filled in a HPMC size 3 capsule and aerosolized into a next generation impactor (NGI) (MSP Corp., Shoreview, MN) using the inhalers at an airflow rate corresponding to a 4 kPa (31) pressure drop across the devices. Capsule piercing was done by hand with two holes positioned near the capsule ends (Fig. 2c). Optimization of capsule aperture size (1.5, 0.8 and 0.5 mm) was performed using the HH device. The powders were aerosolized until a total air volume of 4 L (32) was drawn through the inhalers at ambient conditions (10–45% RH and 20–24°C). It is widely recognized that dry powder inhaler formulations should be protected from the effects of ambient humidity in order to maintain aerosol performance. Powders were stored a desiccator to prevent moisture ingress and aerosolized following brief exposure to environmental RH conditions. It was not expected that this brief exposure would affect aerosolization performance. All measurements were made with three replicates. The stages of the impactor were coated with silicone spray to minimize particle bounce and re-entrainment. The powders were aerosolized with the DPI in a horizontal position. To assess the total aerosol size distribution and in the absence of a lactose carrier, the USP induction port was not used in this research and development study. After aerosolization, the drug retained in the capsule, CC, mouthpiece with 3D array, and collected on the pre-separator, impaction plates and the filter was extracted by washing with deionized water for quantitative HPLC analysis. The cut-off diameters of each stage at a specific airflow rate were calculated using the formula specified in USP 35 (Chapter 601, Apparatus 5).

The loaded AS dose was determined from the initial weight of the powder taken for aerosolization and the measured percent of AS content in the EEG formulation measured by content uniformity. The mass of AS retained on the capsule, CC and mouthpiece was determined and expressed as a percentage of the loaded AS dose. Emitted dose was calculated by subtracting the mass of AS retained in the capsule, CC and mouthpiece from the loaded AS dose. FPF of the EEG formulation ($FPF_{<5\mu m/ED}$) and sub-micrometer FPF ($FPF_{<1\mu m/ED}$) were defined as the percent mass less than 5 μm and 1 μm, respectively, from the mass percent emitted. MMAD, $FPF_{<5\mu m/ED}$ and $FPF_{<1\mu m/ED}$ were calculated from linear regression equations resulting from cumulative percentage mass *vs.* ln(cut-off diameter) of the respective stages on the NGI plots.

High-Speed Photography

The motion of the capsule inside of the chamber was analyzed using a Photron PCI R2 high-speed camera at 2000 frames per second. This helped to show the overall movement of the capsule as well as to determine the number of apparent chamber wall impactions per second. Rapid changes in capsule direction near the wall surface were assumed to be due to contact with the wall and counted as a capsule wall impactions. The impactions were counted for a total of 1,500 frames to determine the total number per second. Three videos were analyzed for each device and the average impactions per second were calculated from the data.

High-Performance Liquid Chromatography (HPLC)

Albuterol sulfate was analyzed using a modular HPLC system (Waters Co., Milford, MA) with a Restek Allure PFP 15×3.2 mm column (Bellefonte, PA) connected to a 2996 PDA detector. An absorption wavelength of 276 nm was used in conjunction with Empower Pro software (Waters Corporation, Milford, MA) for data acquisition and analysis. The column was maintained at 25°C. The analysis was conducted using isocratic analysis with 70:30 ($\%^{v}/_{v}$) methanol-20 mM ammonium formate in water (pH adjusted to 3.4 with 90% formic acid) at a flow rate of 0.75 mL min^{-1} and an injection volume of 100 μL.

Statistical Analysis

In the current investigation, the data was expressed as the mean ± coefficients of variation (CV) based on three replications of each experiment (except for Fig. 5 where standard deviation was used). The statistical significance was determined using one-way analysis of variance with Tukey's post hoc analysis and between the groups using independent

sample *t*-test at a p-value of 0.05 using SPSS (Version 21.0, SPSS, Inc., IL, USA).

RESULTS

Capsule Aperture Size Optimization with the HandiHaler

The effect of capsule aperture size on the EEG formulation aerosol aerodynamic size distribution was determined using the HH at 45 L min^{-1}, which corresponds to a pressure drop of 4 kPa across the device. The HH was selected as a general capsule-based platform that was previously shown to produce good aerosol performance with an EEG formulation (20), and in a separate investigation, it demonstrated uniform sensitivity to deagglomeration irrespective of materials investigated (24). Capsules were pierced by hand with a needle along the major axis where the end curvature started (2 piercings per capsule; see Fig. 2c). Three aperture sizes of 1.5, 0.8 and 0.5 mm were chosen in order to maximize FPF, while minimizing the MMAD. Similar capsule ($p=0.225$; ANOVA) and device ($p=0.069$; ANOVA) retentions were observed with the different aperture sizes. The $FPF_{<1\mu m/ED}$ was significantly higher and the MMAD lower for the 0.5 mm aperture (*t*-test) compared with apertures of 1.5 mm ($p=0.047$ for $FPF_{<1\mu m/ED}$ and $p=0.028$ for MMAD) and 0.8 mm ($p=0.004$ for $FPF_{<1\mu m/ED}$ and $p=0.011$ for MMAD). As the aperture size increased, in general, the CVs increased. The $FPF_{<1\mu m/ED}$ decreased in a quadratic manner ($R^2=0.94$) while MMAD increased in a sigmoid fashion ($R^2=0.90$). Based on these results, the inhalers in this study were tested with a capsule aperture size of 0.5 mm.

Effect of Inlet Air Pattern and Capsule Alignment

The drug deposition and aerosol dispersion efficiency of the five CCs with two air inlets and varying centerline offset distances are presented in Table I. CC_1-3D was used as the control design with air inlets that are inline. Only CC_5-3D showed a significant change, with a decrease in the ED compared to the in-line hole design (CC_1-3D). Similarly, capsule drug retention and mouthpiece retention were similar for each CC except CC_5-3D. For the CC_5 design, the capsule was not observed to move during actuation and this resulted in high capsule drug retention (90.4%). This was because the staggered holes created a stable air pattern that locked the capsule into place resulting in poor ED from the capsule (6.3%) as referenced against loaded dose. Interestingly, for CC_4-3D, the capsule was also observed not to move during actuation; however, the ED and capsule retention were not significantly different from CC_1-3D. Overall, EDs were high with over 60% of the loaded dose being emitted (except CC_5-3D). Excluding CC_5-3D, drug deposition within the mouthpiece was similar for the other four designs, while drug retention in the CCs for CC_1-3D and CC_2-3D appeared lower than CC_3-3D and CC_4-3D (although not reaching statistical significance due the variability in chamber retention observed for CC_4-3D).

In terms of aerosol deagglomeration, measured by $FPF_{<5\mu m/ED}$, $FPF_{<1\mu m/ED}$, and MMAD, each of the inhalers efficiently dispersed the spray dried formulation and a relationship is observed between decreasing dispersion efficiency and increasing offset distance (Table I). The $FPF_{<5\mu m/ED}$ and $FPF_{<1\mu m/ED}$ were significantly lower and the MMAD higher for the CC_5-3D (Fig. 2e) design compared to the control (Table I). For designs CC_1-3D, CC_2-3D and CC_3-3D, the $FPF_{<5\mu m/ED}$ values were above 90%, the $FPF_{<1\mu m/ED}$ values were above 30%, and the MMAD values were less than 1.5 μm, indicating the aerosol dispersed efficiently. It was observed that there was an increase in the aerosol performance variability associated with introducing the staggered hole design to the CC (CC_2-CC_5). The lowest variability was observed for the in-line design (CC_1 - Fig. 2d) for both ED and FPF measurements. Coefficients of variability of 2% or less were reported for the measured ED, $FPF_{<5\mu m/ED}$, $FPF_{<1\mu m/ED}$, and MMAD using the CC_1-3D design.

An additional CC design with a single central hole was also considered, CC_6-3D (Fig. 2f), and the mean (CV) ED with this inhaler was 54.9% (17.5%). Capsule retention and CC drug retention were higher than CC_1-3D and associated with more variability. Aerosol dispersion characteristics were similar to the in-line hole design with mean (CV) $FPF_{<5\mu m/ED}$ and $FPF_{<1\mu m/ED}$ of 93.9% (0.5%) and 34.7% (8.4%), respectively.

In order to observe the motion of the capsule within the CC for different designs, the capsule was visualized and recorded using the high speed camera. Still images of capsule motion at a 4 kPa pressure drop were captured for CC_1-3D, CC_2-3D and CC_3-3D in Fig. 3 at a neutral position and for maximum capsule rocking locations. In general, the capsule movement was in a random pattern where the capsule impacts were observed with the front, back and the side walls of the chamber. From Fig. 3, it can be observed that as the air inlet hole offset distance increased rocking of the capsule along its primary axis also increased. However, this rocking motion does not appear to increase fluidization of the aerosol in a way that leads to improved deagglomeration of the powder.

The number of capsule impactions per second as a function of air inlet hole offset distance from the central axis is provided in Fig. 4 at a 4 kPa pressure drop over the inhalers. As the offset distance of the air inlet holes increased (CC_1-3D to CC_3-3D), the number of capsule impactions with the walls of the CCs per second significantly decreased ($p\leq0.0005$; ANOVA) in a quadratic manner with a strong coefficient of determination ($R^2=0.98$). For comparison, the commercial HH produced 199.6 (3.3) [mean (CV); $n=3$] capsule-to-wall

impactions per second. These results indicate that symmetric inlet flow produces the largest instability in the system, which leads to the highest vibrational frequency and number of wall impacts. Furthermore, the vibrational frequency and associated number of wall impacts appears to be related to improved deagglomeration of the aerosol. Considering that the CC_1-3D inhaler demonstrated statistically equivalent values of ED and MMAD to those of $CCs_{2\text{-}4}$, but had the lowest performance variability of all CCs tested, it was selected for further optimization and evaluation.

Improved Deagglomeration Performance of the 3D Array: Use of Metal Rods

In order to further improve powder deagglomeration, the resin 3D rod array in the mouthpiece was replaced by a metal (stainless steel) 3D rod array to form the CC_1-3Dm inhaler. Both the CC_1-3D and CC_1-3Dm inhalers were tested for aerosolization performance with a new batch of the EEG formulation (batch 2), and results are presented in Table II. The content uniformities ($n=3$; mean ± SD) of AS in batch 1 and 2 powders were 27.0 ± 1.4 and 28.0 ± 0.3%, respectively. The content uniformity compared between the batches was not significantly different ($P=0.268$; *t*-test). Small differences in the performance of CC_1-3D with the resin array are observed between the results presented in Tables I and II. These differences are due to batch to batch variability in the spray dried powder. Despite the use of the same operating conditions with the spray dryer, it is expected that there may be batch to batch variability in the powders produced. The aerodynamic size distributions obtained with these different batches and aerosolization with CC_1-3D inhaler were statistically compared (Table I *vs.* Table II results). Insignificant differences (*t*-test) were observed between these EEG formulation powder batches for the key aerosolization performance parameters: $FPF_{<5\mu m/ED}$ ($p=0.789$), $FPF_{<1\mu m/ED}$ ($p=0.146$) and MMAD ($p=0.218$).

Replacing the resin array (CC_1-3D) with the metal array (CC_1-3Dm) did not alter the resistance of the mouthpiece. In comparing CC_1-3D resin and metal arrays at a 4 kPa pressure drop (50 L min^{-1}), the CC_1-3Dm design demonstrated significantly (*t*-test) lower mouthpiece retention ($p=0.001$), smaller MMAD ($p=0.003$) and higher $FPF_{<1\mu m/ED}$ ($p=0.004$) compared to the resin 3D-array version (Table II). The improved performance of the metal array design was likely due to either increased particle rebound from the metal *vs.* resin surfaces or improved structural integrity of the array with metal construction. The resin array was observed to deform with use due to the extremely small rod diameters (0.5 mm) and high airflow velocities. Despite increased deagglomeration, there was no significant difference in the ED between the CC_1-3D and CC_1-3Dm devices ($p=0.525$; *t*-test).

It was observed that the majority of the mouthpiece retention was a result of powder impaction on the sigmoid curve in the flow passage prior to entering the 3D array, which could be due to capsule orientation and powder release locations from the capsule into the mouthpiece. In an attempt to minimize mouthpiece retention, the distance from the entrance of the mouthpiece to the start of the metal 3D array was increased from 14.5 mm to 29.0 mm, which could potentially reduce particle impaction on the curved wall. However, increasing the length of the mouthpiece did not decrease the mouthpiece retention ($p=0.176$) or improve deagglomeration ($p=0.750$, 0.789, 0.588 for $FPF_{<5\mu m/ED}$, $FPF_{<1\mu m/ED}$ and MMAD, respectively; *t*-test). Therefore, the more compact design of the CC_1-3Dm inhaler was retained. Based on significantly improved powder deagglomeration ($FPF_{\leq 1\mu m/ED}$ & MMAD) and decreased mouthpiece drug retention compared to CC_1-3D, the CC_1-3Dm design was selected for coating the capsule inner surface and inhaler body with PTFE.

Effect of PTFE Surface Modification on Aerosolization Performance

Table II compares the PTFE coated device (CC_1-3Dm-PTFE) with the uncoated resin and metal rod inhalers. Coating the capsule and inhaler has a significant effect on decreasing capsule drug retention, together with decreasing chamber

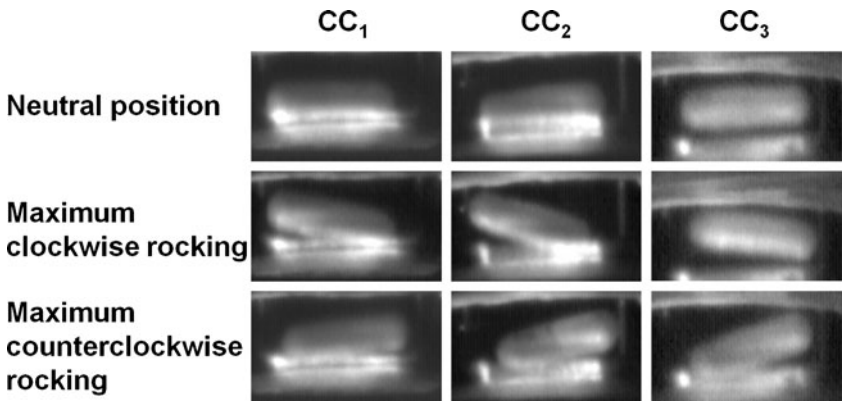

Fig. 3 Still images of capsule motion in the chambers showing an approximate neutral position, maximum clockwise and counterclockwise rocking at a 4 kPa pressure drop using CC-3D inhalers with capsules chambers CC_1, CC_2 and CC_3.

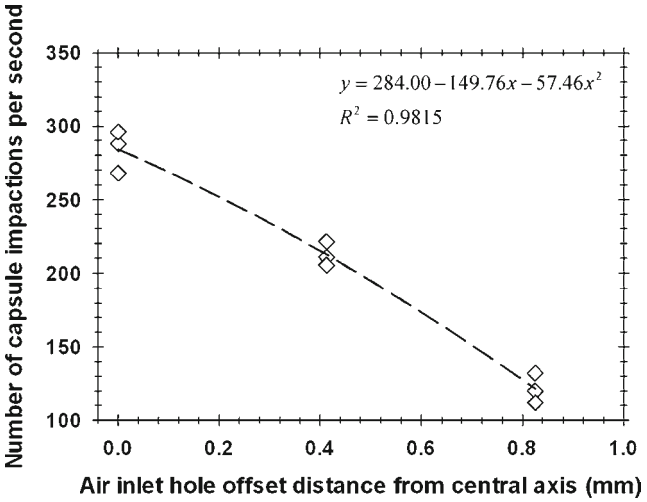

Fig. 4 Number of capsule-wall impactions per second for two air inlets and different inlet hole offset distances. Cases considered were CC_1 (offset from central axis: 0 mm), CC_2 (offset from central axis: 0.4125 mm) and CC_3 (offset from central axis: 0.825 mm).

and mouthpiece retention compared to the original CC_1-3D design. The decreased device drug retention with PTFE coating is reflected in the impressive ED of 81.4% of the loaded dose, which was delivered with low variability (CV = 2.7%). In addition, the coating appeared to maintain the improved aerosolization performance that was previously observed with the metal rod design. There was no significant change in the $FPF_{<5\mu m/ED}$, which was maintained at a high value of 92.7%, while the $FPF_{<1\mu m/ED}$ was higher ($p = 0.004$; *t*-test) and MMAD was lower ($p = 0.002$; *t*-test) than the CC_1-3D design. Comparison of CC_1-3Dm-PTFE with CC_1-3Dm results in similar deagglomeration, but the coated device produces a significantly higher ED ($p \leq 0.0005$; *t*-test). The optimization studies described above have resulted in the CC_1-3Dm design with PTFE coating, which produced $FPF_{<5\mu m/ED}$ and $FPF_{<1\mu m/ED}$ of 92.7% and 36.8%, respectively, an ED of greater than 80% and a final MMAD of 1.3 μm.

Table II Mean Drug Deposition and Aerosolization Performance of CC_1 with Resin or Metal 3D Rod Arrays and with the PTFE Coated Capsule and Inhaler Tested at a 4 kPa Pressure Drop (Equivalent to 50 L/min for Each Inhaler)

Description	CC_1-3D	CC_1-3Dm	CC_1-3Dm-PTFE
Emitted (%)*	63.8 (3.0)	64.7 (2.3)	81.4 (2.7)**
Capsule retention (%)*	14.1 (9.0)	16.2 (4.1)	7.3 (14.2)**
Capsule chamber retention (%)*	8.8 (15.3)	8.8 (11.0)	2.2 (25.4)**
Mouthpiece retention (%)*	13.2 (2.7)	10.2 (3.6)**	9.1 (15.9)**
$FPF_{<5\mu m/ED}$ (%)	93.9 (0.4)	94.5 (0.9)	92.7 (1.3)
$FPF_{<1\mu m/ED}$ (%)*	32.2 (3.2)	37.3 (2.6)**	36.8 (2.3)**
MMAD (μm)*	1.44 (1.96)	1.30 (1.74)**	1.30 (0.97)**

Batch-2 EEG formulation combination particles generated by Büchi Nano Spray Dryer (B-90)

Coefficient of variation (%) is shown in parenthesis [$n = 3$]

*$P < 0.05$ significant effect between uncoated devices built with resin, metal 3D arrays and PTFE coated inhaler device with metal 3D array on % emitted, capsule, capsule chamber & mouthpiece retentions, $FPF_{<1\mu m/ED}$ and MMAD (one-way ANOVA)

**$P < 0.05$ significant difference compared to CC_1-3D with resin rod array (post-hoc Tukey)

Effect of Capsule Coating on Drug Retention

The aerosolization behavior of coated capsules when dispersed into an NGI at a 4 kPa pressure drop using the CC_1-3Dm inhaler is presented in Table III. Coating the capsule with magnesium stearate was observed to decrease the capsule drug retention compared to the uncoated capsule (CC_1-3Dm; Table II). Coating with the EEG formulation and L-leucine had no effect on capsule drug retention compared to the uncoated capsule. Comparing the three coatings, there was no significant difference between the capsule drug retention for the magnesium stearate and L-leucine coatings ($P = 0.085$; *t*-test); an indication that the lubricant's chemical nature may not play a significant role in reducing capsule retention. Coating the capsules with combination EEG particles, L-leucine and magnesium stearate produced insignificant differences (ANOVA) in mouthpiece ($P = 0.594$) and CC_1 ($P = 0.709$) retention. In addition, there were no significant differences (ANOVA) in the aerosol performance characteristics of $FPF_{<5\mu m/ED}$ ($P = 0.082$), $FPF_{<1\mu m/ED}$ ($P = 0.192$) and MMAD ($P = 0.178$). The capsule retention was similar between the L-leucine and magnesium stearate coated capsule; however, the particle size distribution of the lubricants was not determined in this investigation, which may play a key role in detachment/de-agglomeration (33) from the host surface (based on the theories of deagglomeration and detachment from binary & ternary mixtures for inhalation).

Comparison with Commercial Inhalers and a Previously Modified HandiHaler

A recent study of Son *et al.* (20) demonstrated that when the EEG formulation was aerosolized using the capsule chamber of the HH inhaler combined with the 3D rod array design (HH-3D inhaler with rods constructed of resin material) at 45 L min^{-1}, it showed better aerosolization efficiency compared to the AL operated at 80 L min^{-1} and the commercial HH at 45 L min^{-1}. As demonstrated above, small batch to batch variability in the EEG spray dried formulation may result in differences in aerosolization performance. To accurately compare performance of the new inhaler design (CC_1-3Dm-PTFE), these commercial inhalers and the previously developed HH-3D inhaler devices were tested with the same EEG formulation batch. Aerosolization performances for the

AL (80 L min^{-1}), HH (45 L min^{-1}) and HH-3D (45 L min^{-1}) using an optimized EEG formulation (batch 2) were determined with results presented in Fig. 5a–c. There was no statistically significant difference in capsule drug retention (Fig. 5a) between the four devices ($p=0.100$; ANOVA). However, the percentages of EEG formulation emitted from the AL device operated at 80 L min^{-1} and the HH-3D design were lower than both the commercial HH and the CC_1-3Dm-PTFE inhalers. In the case of the AL, decreased ED was due to higher CC drug retention (Fig. 5a). Similarly, the HH-3D device had a lower ED, but in this case it was due to higher mouthpiece drug retention (Fig. 5a), which was reduced by using the PTFE coating for the CC_1-3Dm-PTFE inhaler. In terms of aerosol deagglomeration, each inhaler generated an aerosol with a high $FPF_{<5\mu m/ED}$ (Fig. 5b), all were greater than 80% of the ED. The CC_1-3Dm-PTFE did appear to deagglomerate the submicrometer formulation better than the other devices (Fig. 5b), with the $FPF_{<1\mu m/ED}$ being significantly higher than AL, HH and HH-3D. This resulted in the CC_1-3Dm-PTFE inhaler having the lowest drug aerosol MMAD of 1.30 μm (Fig. 5c).

Table III Effect of Capsule Wall Coatings on the Mean Drug Deposition and Aerosolization Performance of CC_1-3Dm at a 4 kPa Pressure Drop

Description	EEG formulation	L-leucine	Magnesium stearate
Emitted (%)*	65.3 (3.9)	67.8 (2.6)	72.9 (1.6)**
Capsule retention (%)*	14.2 (12.5)	12.7 (10.7)	9.2 (23.9)**
Capsule chamber retention (%)	7.8 (34.1)	6.7 (17.8)	6.9 (7.3)
Mouthpiece retention (%)	12.7 (28.7)	12.9 (10.1)	11.0 (14.6)
$FPF_{<5\mu m/ED}$ (%)	95.4 (0.4)	95.2 (0.7)	94.4 (0.4)
$FPF_{<1\mu m/ED}$ (%)	38.1 (3.7)	36.6 (4.0)	36.0 (1.6)
MMAD (μm)	1.29 (2.75)	1.33 (2.50)	1.35 (0.88)

Batch-2 EEG formulation combination particles generated by Büchi Nano Spray Dryer (B-90)

Coefficient of variation (%) is shown in parenthesis [$n=3$]

*$P<0.05$ significant effect of capsule wall coatings with EEG formulation, L-leucine and magnesium stearate on % emitted and capsule retention (one-way ANOVA)

**$P<0.05$ significant difference compared to capsule wall coated with EEG formulation (post-hoc Tukey)

DISCUSSION

This study has illustrated some of the challenges associated with forming a submicrometer aerosol using a DPI platform. The approach implemented in the current analysis begins with submicrometer spray dried primary particles with geometric diameters of approximately 500–900 nm (19). Completely dispersing this powder into a submicrometer aerosol may not be possible considering the cohesive forces that must be overcome in the very short time of aerosol formation before the particles leave the inhaler. These forces will have a spectrum of strengths with some being almost impossible to break with aerodynamic forces (34,35). Simply making the initial primary particles smaller could reduce the reported aerosol MMAD; however, this approach will increase the polydispersity of the aerosol and could interfere with the final size achieved by condensational growth (13). Fortunately, previous studies have demonstrated that ideal performance with EEG delivery can be achieved using an aerosol that has a small MMAD and maximizing the fraction of particles less than 1 μm. The first goal of EEG delivery is to avoid extrathoracic deposition, with a target value of less than 5% MT depositional loss. Son *et al.* demonstrated deposition in an adult MT model of less than 5% for a 1.4 μm EEG aerosol (19) and less than 3% with a 1.1 μm EEG aerosol (20). Device ED percentages were in the range of 75–80%, which appear acceptable and consistent with state-of-the-art DPI devices (19,20). As a result of these observations, design goals for a high efficiency DPI that can achieve negligible MT deposition are the production of an aerosol with an MMAD of less than 1.5 μm with a $FPF_{<1\mu m/ED}$ above 30%, a $FPF_{<5\mu m/ED}$ above 90%, and an ED of approximately 75% or higher.

A primary outcome of this study is the design evaluation of a capsule positioned perpendicular to the incoming airflow. Factors affecting the formation of an aerosol from a capsule-based device include motion and vibration of the capsule for initial fluidization of the powder (36), airflow inside the capsule (37), and deagglomeration of the aerosol powder in the airstream (21,38,39). It was expected that the perpendicular orientation of the capsule would increase the vibrational frequency and thereby improve initial fluidization of the powder. Based on results, a quantitative correlation was not found between the number of wall impactions and the final MMAD of the aerosol. This is likely because of the multiple factors involved with the aerosolization process, as described above. However, the perpendicular capsule orientation for the symmetric air inlet cases was observed to produce more capsule wall impactions per second (268–296) than with the CC of the HH-3D inhaler (173–184), which orients the capsule parallel to the flow. The perpendicular capsule inhalers (not including the inlet staggered devices) consistently produced a smaller MMAD (1.30 μm – CC_1-3Dm) compared with the parallel capsule alignment cases (1.47 μm – HH-3D). A general trend was also observed where increasing two hole staggering distance reduced the number of wall impactions (Fig. 4) and increased MMAD (Table I). In contrast, the perpendicular capsule alignment devices did not empty as well (ED of 64.7% – CC_1-3Dm) compared with the parallel capsule device (ED of 79.7% with HH). Most likely, the perpendicular oriented capsule improved the vibrational frequency leading to smaller

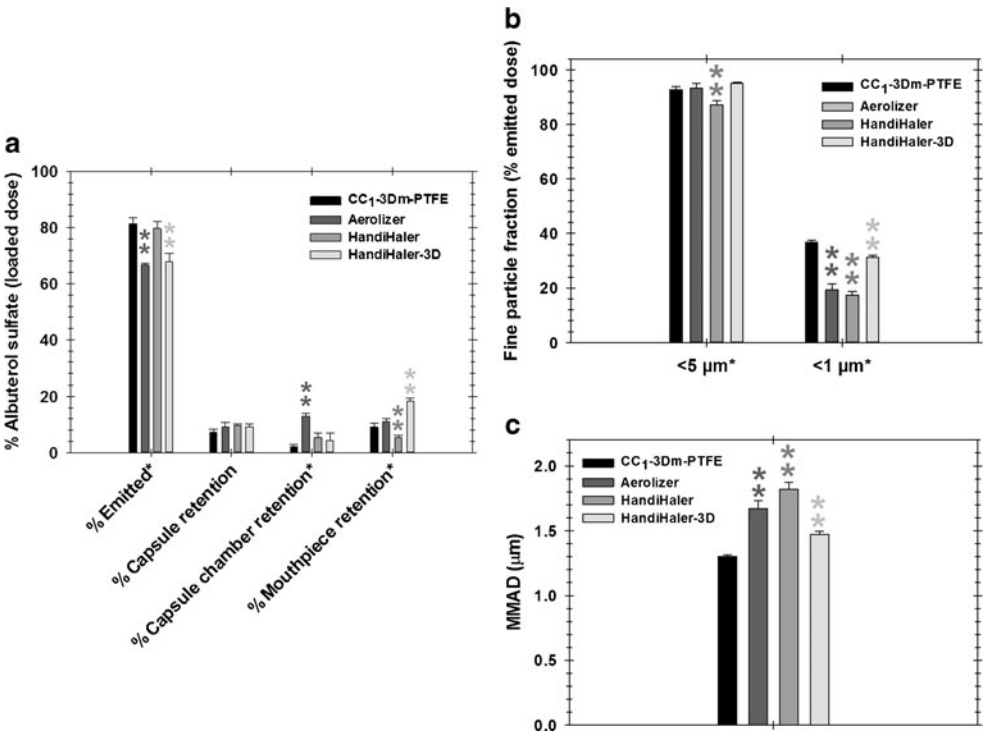

Fig. 5 Comparison of aerosolization performance [$n = 3$; Mean (SD)] of CC_1-3Dm-PTFE with commercial and modified powder inhaler devices (batch 2 powders). (**a**) Percent albuterol sulphate as a function of device and capsule retentions, (**b**) fine particle fractions less than 5 and 1 μm, and (**c**) mass median aerodynamic diameters. *$P < 0.05$ significant effect of inhaler type on % emitted, capsule chamber retention, mouthpiece retention, FPF and MMAD (one way ANOVA). **$P < 0.05$ significant difference compared to CC_1-3Dm-PTFE (post-hoc Tukey).

MMADs, but did not increase airflow through the capsule, which leads to reduced capsule empting. The net result is an improved or similar MMAD with perpendicular capsule alignment but reduced capsule emptying (16.2% retention with CC_1-3Dm from Table II *vs.* 9.6% retention with HH from Fig. 5a) and ED (64.7% with CC1-3Dm *vs.* 79.7% with HH).

Perhaps the largest improvements in inhaler performance observed in this study were gained through the use of surface modifications (Table II). Implementing a stainless steel 3D rod array in the CC_1-3D inhaler significantly decreased MMAD [1.30 (CC_1-3Dm) *vs.* 1.44 µm (CC_1-3D)] and improved $FPF_{<1\mu m/ED}$ [37.3 (CC_1-3Dm) *vs.* 32.2% (CC_1-3D)]. This effect is most likely due to improved structural integrity of the rods. The use of the stainless steel rods also makes the inhaler safer as the metal can be firmly embedded and secured in the inhaler, and will not break apart due to inhalation forces. Coating the capsules with the EEG formulation and L-leucine had little effect on performance (Table III). The lack of an effect with L-leucine was likely because the size of the coating particles was not optimized. Coating with magnesium stearate reduced capsule retention and achieved an ED of approximately 73%. However, it was with PTFE coating that a major improvement in device performance was observed. Emitted dose increased to above 81% with insignificant changes in both FPF and MMAD (CC_1-3Dm-PTFE *vs.* CC_1-3Dm in Table II). This study is one of the first to demonstrate that device and capsule coating can be used to significantly improve the aerosolization performance of an inhaler. The PTFE coating was easy to apply and was simply sprayed onto the internal surfaces and capsule. Delamination of the material after testing and washing was not observed visually. Furthermore, inadvertent inhalation of the PTFE material would likely be biologically harmless. The resulting CC_1-3Dm inhaler with PTFE coating achieves all of the performance variables prescribed for a high efficiency device needed for effective EEG delivery.

Factors that did not improve aerosolization performance were offset of the two air inlets, use of a single air inlet, and increased mouthpiece length. Offsets of the two air inlet holes were considered in order to maximize vibrational frequency. Instead, the occurrence of air inlet hole offset and increasing offset distance progressively decreased the vibrational frequency, which also displayed a general trend of increasing the MMAD for most cases (Table I). As a result, it appears that the greatest capsule instability is created when the flow enters the CC and impinges on the centerline of the capsule in a symmetric manner. For the single inlet hole, capsule impactions with the wall did not appear to occur. This lack of capsule vibration still produced a reasonable aerosol; however, variability in performance was much higher than with two symmetric air inlets. Finally, increasing the mouthpiece length was intended to streamline the design and decrease particle-wall interactions. Previous studies have demonstrated significant reductions in depositional losses with the use of

streamlined designs (40). However, in this study deposition in the inhaler body was not reduced as a result of an increased length and streamlining, which is likely due to turbulence being the primary deposition mechanism.

In the experiments, more than one batch of spray dried powder was employed. A comparison of results (Table I CC_1-3D *vs.* Table II CC_1-3D) demonstrated that there were insignificant changes to aerosolization performance with the new device between these two batches of powder. For CC_1-3D, the % CVs were 0.7, 1.9, 1.22 *vs.* 0.4, 3.2, 1.96 for $FPF_{<5\mu m/ED}$, $FPF_{<1\mu m/ED}$ and MMAD, respectively, with Batch 1 (Table I) *vs.* Batch 2 (Table II). This indicates that the newly proposed device has low variability in its aerosol performance characteristics and that the variability remained low even during batch to batch testing. This improved robustness of the CC_1-3D device may be due to improved initial fluidization associated with increased vibrational frequency or the inclusion of the 3D rod array, which is absent in the commercial HH design.

The optimum device resulting from this study is the CC_1-3Dm with PTFE coating, which produced a 1.30 μm aerosol with a $FPF_{<1\mu m/ED}$ of 36.8% and a $FPF_{<5\mu m/ED}$ greater than 90%, as well as an ED greater than 80%. Furthermore, this device performed better than the previous best devices identified by Son *et al.* (20) and Longest *et al.* (21). For example, using powder generated for this study, the AL and HH inhalers both produced MMADs above 1.60 μm (Fig. 5c). Compared with HH-3D for the same spray dried powder, the CC_1-3Dm-PTFE device produced a significantly smaller MMAD (1.30 *vs.* 1.47 μm) and higher ED (81.4 *vs.* 68.0%). As a result, the newly developed DPI appears ideal for implementing EEG delivery in a highly efficient manner. However, prior to clinical evaluation, the formulation and coating need toxicological evaluations.

Limitations of the current study include the evaluation of a single EEG drug formulation, implementation of a single dose loading, evaluation of a single airflow rate through the device, and single capsule aperture orientation. Different EEG formulations for various drugs may influence the dispersion and performance characteristics of the device. Therefore, optimization studies may need to be performed for different formulations coupled with the CC_1-3Dm inhaler. The amount of powder loaded into the capsule may also influence performance. In the current study, a 2 mg dose of formulation was loaded into each capsule. Increasing this dose weight will likely improve ED (41). The device was developed for the typical inhalation flow and pressure generated by an adult. Inhaler modifications may be required to maintain performance with flow changes associated with disease state or with pediatric patients. Finally, a single capsule aperture orientation was investigated in this study. Investigations are needed to further explore the affect of capsule aperture orientation on powder deagglomeration.

CONCLUSIONS

Current DPIs have low lung delivery efficiencies and high dose variability. This relatively poor performance limits the use of current DPIs to a small number of inexpensive medications with broad therapeutic windows and minor side effects. The expanded implementation of DPI technologies to next-generation medications as well as pediatric and other sub-populations requires improved delivery efficiency and reduced dose variability. Results of this study describe multiple new strategies for improving DPI performance in terms of high FPF and ED and low MMAD, which are expected to reduced mouth-throat deposition and increase lung delivery. Specifically, the newly proposed capsule orientation and capsule motion pattern reduced or resulted in equivalent MMADs exiting the device compared with commercial and previously explored high efficiency DPIs. As a result, the proposed capsule orientation provides a novel and effective approach for capsule-based inhalers. Airflow within the capsule was likely reduced with the perpendicular orientation, which decreased ED. The use of metal rods in the 3D array improved inhaler performance by significantly reducing aerosol size. Coating the inhaler and capsule with low surface energy PTFE resulted in significantly improved ED. The final CC_1-3Dm device with PTFE coating was the only inhaler considered in this study to meet the specific design requirements for high efficiency EEG formulation delivery. Furthermore, the device was found to be more robust than the considered commercial devices in terms of aerosol performance for different batches of spray dried powder. Future studies are needed to verify low deposition in the MT for the new DPI design, investigate other formulations and dosages, and optimize the device for disease states and pediatric patients.

ACKNOWLEDGMENTS AND DISCLOSURES

This study was supported by Award Number R01 HL107333 and R21 HL104319 from the National Heart, Lung, and Blood Institute. The content is solely the responsibility of the authors and does not necessarily represent the official views of the National Heart, Lung, and Blood Institute or the National Institutes of Health.

REFERENCES

1. Islam N, Cleary MJ. Developing an efficient and reliable dry powder inhaler for pulmonary drug delivery—a review for multidisciplinary researchers. Med Eng Phys. 2012;34:409–27.
2. Newman SP, Busse WW. Evolution of dry powder inhaler design, formulation, and performance. Respir Med. 2002;96:293–304.

3. Smith IJ, Bell J, Bowman N, Everard M, Stein S, Weers JG. Inhaler devices: what remains to be done? J Aerosol Med Pulm D. 2010;23:S25–37.
4. Brain JD, Blanchard JD. Mechanisms of particle deposition and clearance. In: More'n F, Dolovich MB, Newhouse MT, Newman SP, editors. Aerosols in medicine: principles, diagnosis and therapy. New York: Elsevier; 1993. p. 117–56.
5. DeHaan WH, Finlay WH. Predicting extrathoracic deposition from dry powder inhalers. J Aerosol Sci. 2004;35:309–31.
6. Delvadia R, Hindle M, Longest PW, Byron PR. *In vitro* tests for aerosol deposition. II: IVIVCs for different dry powder inhalers in normal adults. J Aerosol Med Pulm D. 2012;26:138–44.
7. Delvadia R, Longest PW, Byron PR. *In vitro* tests for aerosol deposition. I. Scaling a physical model of the upper airways to predict drug deposition variation in normal humans. J Aerosol Med Pulm D. 2012;25:32–40.
8. Zhang Y, Gilbertson K, Finlay WH. *In vivo-in vitro* comparison of deposition in three mouth-throat models with Qvar and Turbuhaler inhalers. J Aerosol Med. 2007;20:227–35.
9. Geller DE, Weers J, Heuerding S. Development of an inhaled dry-powder formulation of Tobramycin using PulmoSphereTM technology. J Aerosol Med Pulm D. 2011;24:175–82.
10. Weers JG, Bell J, Chan HK, Cipolla D, Dunbar C, Hickey AJ, *et al.* Pulmonary formulations: what remains to be done? J Aerosol Med Pulm D. 2010;23:S5–23.
11. Hindle M, Longest PW. Condensational growth of combination drug-excipient submicrometer particles for targeted high-efficiency pulmonary delivery: evaluation of formulation and delivery device. J Pharm Pharmacol. 2012;64:1254–63.
12. Longest PW, Tian G, Li X, Son Y-J, Hindle M. Performance of combination drug and hygroscopic excipient submicrometer particles from a softmist inhaler in a characteristic model of the airways. Ann Biomed Eng. 2012;40:2596–610.
13. Longest PW, Hindle M. Numerical model to characterize the size increase of combination drug and hygroscopic excipient nanoparticle aerosols. Aerosol Sci Technol. 2011;45:884–99.
14. Longest PW, Hindle M. Condensational growth of combination drug-excipient submicrometer particles: comparison of CFD predictions with experimental results. Pharm Res. 2012;29:707–21.
15. Tian G, Longest PW, Li X, Hindle M. Targeting aerosol deposition to and within the lung airways using excipient enhanced growth. J Aerosol Med Pulm D. 2013. doi:10.1089/jamp.2012.0997.
16. Chan H-K. Dry powder aerosol delivery systems: current and future research directions. J Aerosol Med. 2006;19:21–7.
17. Chan H-K. Dry powder aerosol drug delivery—opportunities for colloid and surface scientists. Colloids Surf A. 2006;284–285:50–5.
18. Hickey AJ, Concession NM, Van Oort M, Platz M. Factors influencing the dispersion of dry powders as aerosols. Pharm Technol. 1994;8:58–82.
19. Son Y-J, Longest PW, Hindle M. Aerosolization characteristics of dry powder inhaler formulations for the excipient enhanced growth (EEG) application: effect of spray drying process conditions on aerosol performance. Int J Pharm. 2013;443:137–45.
20. Son Y-J, Longest PW, Hindle M. Evaluation and modification of commercial dry powder inhalers for the aerosolization of submicrometer excipient enhanced growth (EEG) formulation. Eur J Pharm Sci. 2013;49:390–9.
21. Longest PW, Son Y-J, Holbrook L, Hindle M. Aerodynamic factors responsible for the deaggregation of carrier-free drug powders to form micrometer and submicrometer aerosols. Pharm Res. 2013;30:1608–27.
22. Behara SRB, Kippax P, Larson I, Morton DAV, Stewart P. Kinetics of emitted mass—a study with three dry powder inhaler devices. Chem Eng Sci. 2011;66:5284–92.
23. Behara SRB, Larson I, Kippax P, Morton DAV, Stewart P. The kinetics of cohesive powder de-agglomeration from three inhaler devices. Int J Pharm. 2011;421:72–81.
24. Behara SRB, Larson I, Kippax P, Stewart P, Morton DAV. Insight into pressure drop dependent efficiencies of dry powder inhalers. Eur J Pharm Sci. 2012;46:142–8.
25. Podczeck F. Evaluation of the adhesion properties of salbutamol sulphate to inhaler materials. Pharm Res. 1998;15:806–8.
26. Selvam P, McNair D, Truman R, Smyth HD. A novel dry powder inhaler: effect of device design on dispersion performance. Int J Pharm. 2010;401:1–6.
27. Donovan MJ, Smyth HDC. Influence of size and surface roughness of large lactose carrier particles in dry powder inhlaer formulations. Int J Pharm. 2010;402:1–9.
28. Tuli RA, George GA, Dargaville TR, Islam N. Studies on the effect of the size of polycaprolactone microspheres for the dispersion of salbutamol sulfate from dry powder formulations. Pharm Res. 2012;29:2445–55.
29. Heng D, Lee SH, Ng WK, Chan H-K, Kwek JW, Tan RBH. Novel alternatives to reduce powder retention in the dry powder inhaler during aerosolization. Int J Pharm. 2013;452:194–200.
30. Clark AR, Hollingworth AM. The relationship between powder inhaler resistance and peak inspiratory conditions in healthy volunteers—implications for *in vitro* testing. J Aerosol Med. 1993;6:99–110.
31. Ganderton D, Byron PR. Harmonising inhaler testing across the pharmacopoeias. In: Dalby RN, Byron PR, Farr SJ, editors. RDD V. Pheonix: Interpharm Press; 1996. p. 283–92.
32. Hindle M, Jashnani RN, Byron PR. Dose emissions from marketed inhalers: influence of flow, volume and environment. In: Byron PR, Dalby RN, Farr SJ, editors. RDD IV. Richmond: Interpharm Press; 1994. p. 137–42.
33. Behara SRB, Kippax P, McIntosh MP, Morton DAV, Larson I, Stewart P. Structural influence of cohesive mixtures of salbutamol sulphate and lactose on aerosolisation and de-agglomeration behaviour under dynamic conditions. Eur J Pharm Sci. 2011;42:210–9.
34. Behara SRB, Larson I, Kippax P, Morton DAV, Stewart P. An approach to characterising the cohesive behaviour of powders using a flow titration aerosolisation based methodology. Chem Eng Sci. 2011;66:1640–8.
35. Wen HY, Kasper G. On the kinetics of particle reentrainment from surfaces. J Aerosol Sci. 1989;20:483–98.
36. Coates MS, Fletcher DF, Chan HK, Raper JA. The role of capsule on the performance of a dry powder inhaler using computational and experimental analyses. Pharm Res. 2005;22:923–32.
37. Shur J, Lee S, Adams W, Lionberger R, Tibbatts J, Price R. Effect of device design on the *in vitro* performance and comparability for capsule-based dry powder inhalers. AAPS J. 2012;14:667–76.
38. Coates MS, Chan HK, Fletcher DF, Raper JA. Influence of air flow on the performance of a dry powder inhaler using computational and experimental analyses. Pharm Res. 2005;22:1445–53.
39. Voss A, Finlay WH. Deagglomeration of dry powder pharmaceutical aerosols. Int J Pharm. 2002;248:39–50.
40. Longest PW, Golshahi L, Hindle M. Improving pharmaceutical aerosol delivery during noninvasive ventilation: effects of streamlined components. Ann Biomed Eng. 2013;41:1217–32.
41. Lalor CB, Tepper JS, Froland WA. Pharmaceutical polypeptide dry powder aerosol formulation and method of preparation. In PCT/US, editors; 2009; WO2009009775 A1.